Advanced Drug Delivery Reviews 85 (2015) 100–109

Contents lists available at ScienceDirect

Advanced Drug Delivery Reviews

journal homepage: www.elsevier.com/locate/addr

Imaging regional lung function: A critical tool for developing inhaled antimicrobial therapies ☆

Stephen Dubsky, Andreas Fouras *

Department of Mechanical & Aerospace Engineering, Monash University, Victoria 3800, Australia

ARTICLE INFO

Article history:
Accepted 20 March 2015
Available online 27 March 2015

Keywords:
Respiratory infection
Phase contrast
X-ray imaging
Functional imaging
Computed tomography
Deposition

ABSTRACT

Alterations in regional lung function due to respiratory infection have a significant effect on the deposition of inhaled treatments. This has consequences for treatment effectiveness and hence recovery of lung function. In order to advance our understanding of respiratory infection and inhaled treatment delivery, we must develop imaging techniques that can provide regional functional measurements of the lung.

In this review, we explore the role of functional imaging for the assessment of respiratory infection and development of inhaled treatments. We describe established and emerging functional lung imaging methods. The effect of infection on lung function is described, and the link between regional disease, function, and inhaled treatments is discussed. The potential for lung function imaging to provide unique insights into the functional consequences of infection, and its treatment, is also discussed.

Contents

1. Introduction

Respiratory infection has a profound effect on lung function. Subsequently, altered lung function has a significant impact on the delivery of inhaled treatments. Our ability to understand and treat respiratory infection would be greatly enhanced by the ability to consider the regional functional consequences of respiratory infection, and how this

☆ This review is part of the *Advanced Drug Delivery Reviews* theme issue on "Inhaled antimicrobial chemotherapy for respiratory tract infections: Successes, challenges and the road ahead".

* Corresponding author.
E-mail addresses: Stephen.dubsky@monash.edu (S. Dubsky), Andreas.Fouras@monash.edu (A. Fouras).

http://dx.doi.org/10.1016/j.addr.2015.03.010

may affect inhaled treatment delivery. Lung function has traditionally been assessed using spirometry; by measuring the flow of gas at the mouth, the function of the lungs as a whole is calculated. However, the effects of disease on lung function are predominantly restricted to local regions within the lung, providing motivation for the development of imaging methods capable of providing regional lung function measurements. Functional lung imaging has the potential to address unanswered questions of lung pathophysiology [1], and to provide new insight into the development of inhaled treatments of lung disease [2].

In this review we establish the benefit of functional lung imaging in the assessment and treatment of respiratory infection. The main focus is to describe established and emerging functional lung imaging methods, with specific focus on those that may be used in lung function measurement in respiratory tract infection and for development and assessment of inhaled treatments. Table 1 summarizes the different techniques discussed, including advantages and limitations of each. The effect of infection on lung function is described, and the link between regional disease, function, and inhaled treatments is discussed. The potential for lung function imaging to provide unique insights into the functional consequences of infection, and its treatment, is also discussed.

1.1. Lung function in infection and disease

Breathing is a mechanical process where the respiratory muscles work together to produce driving pressures to expand and draw air into the lung for gas exchange [3]. The flow of air inside the lungs, and hence the regional ventilation and function, is determined by mechanical properties, most notably the resistance and compliance. The driving pressure across the respiratory system needs to overcome the total pulmonary resistance against the flow, the static elastic recoil of the alveolar tissue and the thoracic cage against the increasing volume, and also the inertial force of the gas motion.

Fig. 1 shows the basic anatomical elements of the lungs. During inspiration, the dome-shaped diaphragm contracts and flattens, enlarging the thoracic cavity resulting in a decrease of both the pleural pressure and the alveolar pressure inside the lung. This establishes a positive pressure gradient along the airway tree causing airflow into the lung. During expiration, the diaphragm relaxes, and gas is expelled from the lung due to elastic recoil of the lung tissue and chest wall.

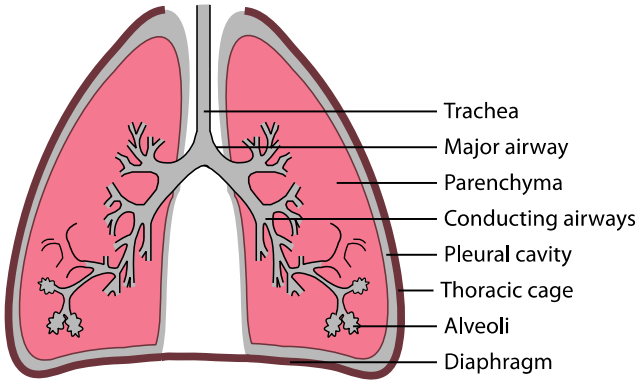

Fig. 1. Basic anatomical elements of the lungs. During inspiration, the diaphragm contracts and flattens, enlarging the thoracic cavity resulting in a decrease in pressure in the pleural cavity. This in turn expands the lungs, reducing pressure in the alveoli causing gas to be drawn in through the trachea and conducting airways.

The lung contains structures that cover a range of scales in order to deliver air to a large surface area for gas exchange [4]. The airways exhibit a branching geometry in which elements are interdependent [5]. Emergent behavior and internal feedback mechanisms mean that while local effects must be resolved, the entire respiratory system must be interrogated as a whole, and the response of isolated tissue may not easily predict whole organ response, for example when airways are constricted in asthma [6–10]. Imaging is well placed to deliver this detailed, yet holistic view of lung function *in situ*.

Disease and infection alter the mechanical properties within the lung, leading to regional alterations in lung function. For example, pulmonary fibrosis will alter the compliance of the lung parenchyma, leading to regional alterations in tissue expansion, even in the very early stages of the disease [11]. Asthma results from airway hyperresponsiveness. Exacerbations occur whereby the airways constrict and narrow, causing an increase in airway resistance that can lead to difficulty breathing and regional ventilation defects [5,6,8,12–14]. Inflammation associated with chronic obstructive pulmonary disease (COPD) leads to the destruction of elastin, which reduces lung elasticity. This results in less elastic recoil (increased compliance) reducing the ability to empty the lungs, and decreasing peak expiratory flow [15].

Table 1
Established and emerging lung imaging methods.

Section	Modality	Advantages	Limitations
Established methods			
2.1	Computed tomography	High spatial resolution	High radiation dose Limited functional information No dynamic information
2.2	4DCT registration-based ventilation	Regional functional measurement High spatial resolution	Very high radiation dose
2.3	Hyperpolarized MRI	Regional functional measurement Zero radiation dose	High cost Lower resolution Limited availability
2.4	Electrical impedance tomography	Bedside imaging High temporal resolution Regional functional measurement Zero radiation dose	Very low resolution
2.5	Nuclear Imaging methods	Regional functional measurement Deposition measurement	Poor temporal resolution High cost Logistically challenging contrast agent required
Emerging functional imaging			
3.2	Grating interferometry	Very sensitive to changes in lung structure	Very poor temporal resolution Challenging imaging setup
3.3	Propagation-based phase contrast imaging	Simple to implement Dynamic imaging High contrast within lung tissue	Less sensitive to phase contrast Requires highly coherent X-rays
3.4	Functional lung imaging using phase contrast	Regional functional measurement Dynamic information	Currently requires highly coherent X-rays
3.5	Laboratory PBI	Improved access for researchers	Under development

Infections of the respiratory tract result in various pathophysiological changes in the lung that lead to altered lung function. Infection with *Legionella pneumophila* bacteria has been shown to cause alveolar wall thickening, edema, focal pneumonia, and lung injury over the course of infection in mice [16]. Patients with cystic fibrosis are particularly susceptible to *Pseudonomas aeruginosa* infection. The resulting inflammatory response proceeds to cause increased secretions, bronchial constriction, pneumonia and damage to the lung parenchyma [17–19]. As a result, typical spirometric lung function metrics, including peak expiratory flow and tidal volume, are reduced over the course of the infection [20,21]. Pulmonary infection with *Listeria monocytogenes* similarly shows inflammatory responses in mice [22]. Bacterial infection, in particular *Haemophilus influenzae*, has been linked to exacerbations in patients with COPD [23,24]. This leads to inflammatory changes and significantly reduced lung function.

It is clear that inflammatory responses and structural changes resulting from pulmonary infection lead to an overall reduction in lung function. Many of these effects are regional and global measurements such a spirometry will fail to show the details of these effects.

Pulmonary infection is typically treated using inhaled antibiotics. The effectiveness of this treatment is dependent on local concentrations of the inhaled agents, which will be dramatically affected by local lung function and airflow [2,25]. This link between regional lung function and effectiveness of inhaled treatment is explored in the following section.

1.2. Assessment of inhaled treatments using functional lung imaging

Airflow is not uniform throughout the lung, and the regional nature of most lung disease can increase this heterogeneity. When some regions of the lung are diseased and underperforming, healthy regions may compensate, masking the disease from global functional measures such as spirometry [11,26]. Assessment of treatment outcomes using global lung function measures will be similarly hindered, a major challenge for development of novel drugs and delivery mechanisms.

The effectiveness of inhaled treatments for lung diseases is significantly affected by the deposition distribution within the lung. This is determined by two categories of factors: particle related factors, such as shape, size, density and concentration of the inhalant, and patient related factors that relate directly to airflow [25]. These patient-related factors include airway obstructions, which cause local flow changes that increase inhalant deposition at the obstruction site, and alterations in tissue expansion due to disease that cause preferential airflow to healthy regions of the lung [25] and hence more inhalant deposition in these regions [27]. Therefore, the underlying functional deficit due to disease, the site of deposition, and the functional recovery due to treatment form a feedback loop that dramatically influences the effectiveness of treatment (Fig. 2). Measurement of local lung function would provide new insight into these interactions, improving our understanding of the physiological consequences of lung infection, but also the factors that influence effective inhaled delivery of treatments.

Imaging is underutilized in pharmaceutical drug development, with imaging performed on only about 1% or 2% of animals used in the preclinical stages of drug development [28]. Development of truly functional imaging methods would harness the power of regional measurements and provide added sensitivity and information for assessment of novel treatments.

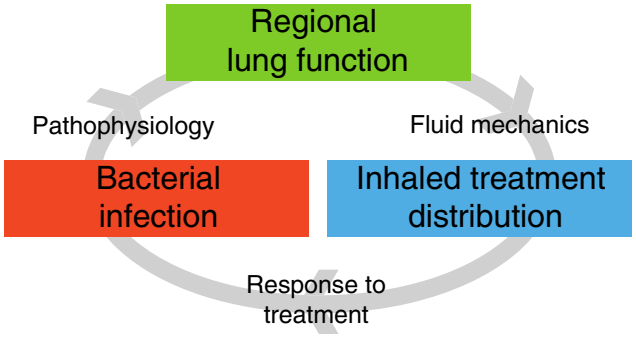

Fig. 2. Feedback in inhaled treatment of respiratory infections. Regional lung function, inhaled treatment distribution and bacterial infection form a feedback loop, whereby lung function, which is altered due to the underlying pathology, determines the inhaled treatment distribution, which strongly influences the treatment effectiveness and hence pathological response.

1.3. Use of imaging for investigation into inhaled treatment deposition

The distribution of deposition within the lung of an inhaled treatment agent clearly has a large influence on the effectiveness of that treatment. It is important, therefore, to separate the effect of the delivery mechanism from the pharmacological action to accurately assess its suitability. An otherwise viable treatment may be ineffective if the antibiotic is not delivered in sufficient concentration to the infected areas within the lung. This may cause direct detriment to the patient, and may also lead to a potentially viable pharmaceutical treatment being rejected during development due to apparent ineffectiveness.

During inspiration, gas flow reduces in the lung through each successive bifurcation generation, as the flow is divided between more and more airway branches. Turbulence, separated flow, and recirculation may occur in the proximal airways, particularly around airway bifurcations. Larger and denser particles preferentially deposit on the inner wall downstream of the first few bifurcations, as their greater inertia causes them to impact the airway wall in these regions. As the flow rate reduces through each generational branching, the flow becomes increasingly laminar, and diffusion becomes the predominant gas mixing mechanism in the distal airways. Deposition mechanisms that predominate in smaller airways are gravitational sedimentation,

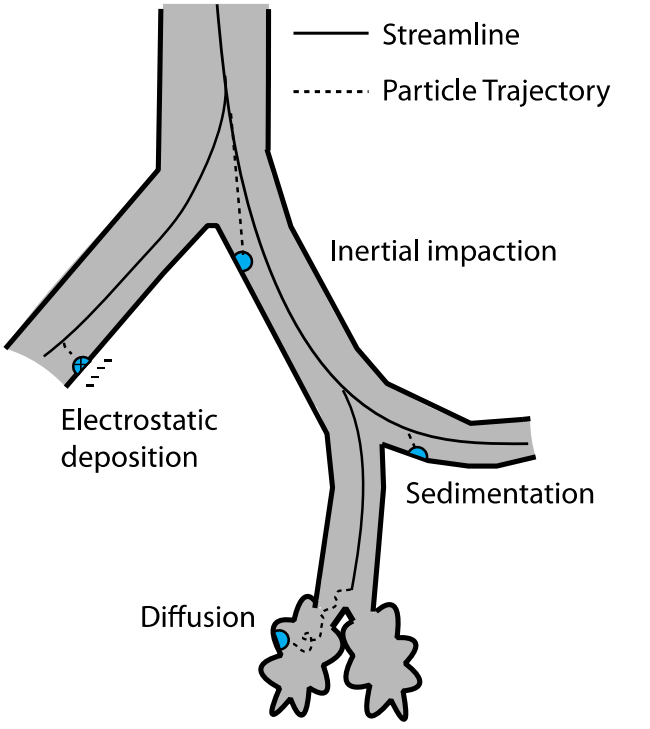

Fig. 3. Various inhalant deposition mechanisms. In high flow regions, inertia causes larger particles to impact the airway wall, whereas smaller particles tend to deposit in distal airways due to diffusion, sedimentation or electrostatic forces.

and diffusive and electrostatic deposition (Fig. 3). A percentage of smaller particles traverse the lung without depositing to be expelled upon exhalation. In this way, the fluid mechanics and particle properties interact to determine the site of deposition.

A significant challenge in determining the interaction between local function and inhaled deposition lies in the fact that regional airflow, the major factor in deposition distribution, is difficult to measure *in vivo*. Although recent advances in functional imaging are addressing this challenge, widespread use of these methods has not yet been achieved. An additional challenge is that directly measuring inhalant deposition non-invasively at high resolution is difficult to achieve. The most widely used imaging method for determination of regional particle deposition has been nuclear imaging. In this method, a radionuclide contrast agent is inhaled into the lung, and the emitted high energy radiation is imaged using gamma detectors to provide local concentration measurement of the inhaled agent [29]. This can provide regional measurement of deposition. However, spatial resolution is not sufficient to localize deposition measurement to specific airway locations. These two challenges mean that directly correlating airflow with inhaled treatment deposition experimentally has been thus far unachievable.

The lack of acceptable experimental data has necessitated a focus on computer simulation to investigate the various factors that contribute to particle deposition. Although effective for fundamental studies of deposition, for computer simulation to accurately predict inhaled treatment deposition, detailed knowledge of airway geometry and pressure/flow inputs in both health and disease are required. As these data are not readily available, investigators must often resort to assumptions that can drastically influence results, reducing the ability of simulations to accurately reflect the real-world situation [30–32].

A common assumption is that the airway tree is rigid and static. Often the geometry of the airway tree is measured from computed tomography (CT) images acquired during a breath-hold maneuver [33–38]. Mead-Hunter et al. (2013) [30] studied the effect of the static airway geometry simplification on deposition distributions calculated from numerical modeling. Significant differences in the predicted deposition patterns were found between the simulations using a dynamic (moving) airway geometry compared with those simulated using a static airway tree. This highlights the sensitivity of inhalant deposition to dynamic effects, and demonstrates the importance of including dynamics in deposition modeling.

As an additional input into computer simulations of particle deposition, several studies have used changes in lobar volume measured from CT images at two phases of the breathing cycle, to estimate the flow into peripheral airways [33,36,37]. Steady flow is often imposed between these two phases, which are typically chosen to be functional residual capacity and total lung capacity. Although an improvement over spatially uniform pressure/flow simplifications, this method does not take into account dynamic effects throughout the respiratory cycle that may affect inhaled treatment distribution, and also neglects intra-lobar variability.

The emerging dynamic imaging methods described in this review can provide invaluable information for modeling studies. This will obviate many of the assumptions and simplifications currently employed, resulting in much improved deposition distribution simulations for study and optimization of inhaled treatments.

2. Established lung imaging methods

There are several imaging methods that are well developed for the lung. Although these provide very useful information, there are several capability limitations that hinder use in particular situations. In this section we provide an overview, explain the technical principles, and describe the advantages and disadvantages of each technology. Our goal is to provide a working knowledge of the capabilities of each imaging mode, allowing assessment of their potential for use in investigations into pulmonary infection and inhaled treatments.

2.1. Computed tomography

The current gold standard for lung imaging is computed tomography (CT), which is capable of providing high-resolution three-dimensional images of the internal structures of the lung. To achieve this, X-ray images are acquired from multiple viewing angles. These projections represent line integrals of the X-ray transmission of the sample from different angular orientations. The three-dimensional lung structure is reconstructed from these projections using back-projection or iterative methods [39]. The spatial resolution of the projections and the number of viewing angles used in the reconstruction determines the resulting spatial resolution of the reconstruction. Therefore, a high-resolution CT scan requires many high-resolution projection images to be acquired.

CT scanners predominantly employ a single source and detector pair that is rotated around the subject to collect the required projection data. Movement of the subject during a scan results in artifacts in the reconstruction that degrade image quality and spatial resolution. Therefore, CT is best performed on stationary objects. To reduce these artifacts in the case of lung imaging, CT scans of the lungs are typically acquired during a breath-hold maneuver.

As with all X-ray based imaging methods radiation dose is a significant concern when using computed tomography *in vivo*. The ionizing nature of absorbed X-rays can damage DNA, either directly, or through the creation of free-radicals. For this reason, X-ray dose significantly increases the probability of developing cancerous tumors. It is therefore necessary to minimize radiation dose in X-ray imaging methods. This factor is most critical in CT, where the use of many X-ray projection images results in high radiation exposure [40]. The requirement for minimization of dose means that it is difficult to perform repeated imaging at high resolution to investigate the progression of infection, or to monitor the effectiveness of inhaled treatments over time.

Xenon gas may be used as a contrast agent and combined with washout techniques to determine regional ventilation [41,42]. However, this requires serial CT imaging, significantly increasing X-ray dose. Additionally, as the density and viscosity of Xenon gas is much greater than air, the distribution of Xenon gas may not accurately reflect the regional ventilation of respiratory gases under normal conditions [42].

Nevertheless, CT has the ability to provide measurement of lung health in a variety of conditions. For example, Galbán et al. [43] used changes between two CT reconstructions (one at end inspiration, and one at end expiration) as a surrogate biomarker for chronic obstructive pulmonary disease. Using this method they were able to assess the regional severity of the disease. De Langhe et al. [44] quantified lung fibrosis and emphysema in mice using computed tomography. Wielputz et al. [45] utilized a low-dose computed tomography method to monitor cystic fibrosis lung disease in mice over time. Kobayashi et al. [46] utilized micro-computed tomography to assess emphysema in a COPD exacerbation mouse model.

CT can be utilized to provide either an indirect assessment of lung health through biomarkers, or a direct measurement of lung health where structural changes in lung tissue can be resolved. Unfortunately, many lung diseases may produce significant functional changes for only subtle changes in lung structure that may not be readily deduced from static CT imaging.

2.2. Ventilation measurement using 4DCT registration-based methods

The motion of lung tissue is integrally connected to its function. The flow of air into a region of the lung results from the expansion of that tissue, and hence measurement of lung tissue expansion over the breathing cycle allows inference of regional airflows throughout the lung.

CT has been combined with image registration techniques to provide measurement of lung motion. Image registration is an image processing method that allows matching of the spatial location of a landmark or object between two separately acquired images. Several studies have

used image registration to measure the motion of lung tissue between two volumetric lung images acquired using CT in two breath-hold states [47–50]. Unfortunately, data acquired in this way does not truly capture the dynamics of breathing.

An alternative approach that provides dynamic imaging exploits the periodic motion of the lung during the breathing cycle. Respiratory gating is used to sort projection data into specific phases of the breath, allowing phase-averaged 4DCT of the lung to be performed at various points in the breathing cycle. Several studies have combined 4DCT with image registration to measure lung motion and regional ventilation during the breathing cycle [51–53]. These data can be used to assess the health of the lung tissue. For example, Yamamoto et al. [54] demonstrated this technique for measurement of regional disease in patients with emphysema.

The major limitation for this approach is a requirement to expose the subject to high radiation dose. 4DCT-based measurement of ventilation requires at least one additional CT scan to be acquired for each time-point measured, multiplying the dose required dramatically. The high radiation dose makes serial imaging impractical and limits the use of 4DCT to subjects where the significant risks of large radiation dose are acceptable: for example, patients with advanced disease or preclinical models.

2.3. Hyperpolarized magnetic resonance imaging

Magnetic resonance imaging (MRI) utilizes the radiofrequency signals emitted by polar nuclei when their spin is modified by an externally applied magnetic field in order to generate 3D images of biological subjects. Hydrogen atoms contain polar nuclei and are found in abundance in soft tissue, providing an ideal material for imaging with MRI. However, the inflated lung is approximately 80% air, and the resulting low tissue density within the lung results in poor image quality. To overcome this problem, hyperpolarized noble gases have been produced that enhance the MRI signal by several orders of magnitude when inhaled. Regional variation in ventilation distribution can be obtained, because the signal is proportional to the concentration of gas within the lung regions [55]. Additionally, by utilizing specialized magnetizing sequences, other functional measurements may be performed such as lung microstructure, oxygenation and perfusion [56], although with varying degrees of success.

MRI imparts no radiation dose, a major advantage over X-ray based imaging methods. However, despite recent improvements, the resolution is still significantly lower than CT.

Despite recent advances, there exist a number of challenges hindering widespread use of hyperpolarized MRI [56]. Cost is the most significant factor. The production of hyperpolarized gases is expensive, and the limited half-life of these gases causes significant logistical issues. Additionally, highly specialized and expensive technology is required to produce the necessarily strong magnetic fields used for imaging the hyperpolarized gases [57]. Perhaps due to the prohibitive cost of hyperpolarized MRI, no substantial study has yet demonstrated the relative sensitivity and specificity advantages of this method over other modalities.

2.4. Electrical impedance tomography

The electrical impedance of regions within the chest will vary depending on the proportion of the various constituents. The proportions of blood, tissue, and air in the chest cavity will vary both spatially and over the respiratory and cardiac cycles. Electrical impedance tomography (EIT) uses the varying impedance in the chest to measure changes in ventilation and perfusion during breathing [58–60].

In EIT, electrodes are placed around the chest, and voltage profiles are collected for all drive and receive electrode–pair combinations. Tomographic methods are used to reconstruct the time varying electrical properties within the lungs during breathing, allowing the proportion of blood, tissue and air inside the chest to be mapped, and regional ventilation and perfusion to be calculated. Electrical impedance tomography has many advantages for clinical application. The simple and compact hardware required are well suited to measurement at the bedside. However, EIT is fundamentally limited by maximum number of electrode/detector pairs that can be practically used, resulting in an ill-posed reconstruction problem and spatial resolutions far lower than CT or MRI based modalities [58].

EIT is a useful clinical tool for monitoring the lung function of patients. However, for investigation into respiratory infection and inhaled treatments where smaller scale functional changes are important, the lack of spatial resolution limits the utility of EIT.

2.5. Nuclear medical imaging

Nuclear medical imaging methods utilize the detection of gamma-ray photons emitted by radioactive contrast agents within a subject. The radiolabeled substance is used to preferentially target an organ or disease process. There are three major imaging modes that are categorized as nuclear medical imaging: gamma scintigraphy, positron emission tomography (PET), and single photon emission computed tomography (SPECT).

Although localization of the labeled pharmaceutical compound to specific areas can provide excellent contrast, nuclear medicine techniques generally suffer from poor signal-to-noise as the amount of radioactive material must be minimized for the safety of the subject. Although spatial resolutions have improved dramatically over the past decade, temporal resolution remains poor [61].

Nuclear medicine enables studies of lung function to be carried out, including the determination of regional ventilation and gas exchange [13, 63–64]. For functional lung imaging, this radioactive agent is inhaled into the lungs. Functional lung measurements using nuclear imaging are well suited for testing of efficacy of inhaled treatments to provide a measure of a treatment success from a functional, as opposed to anatomical, perspective. Additionally, the functional data obtained may be used as a validation for numerical simulation [33].

Radionuclide agents can be tagged to specific materials, and consequently nuclear imaging can be used to directly track deposition of pharmaceutical compounds into the lung – a highly useful tool for inhaled treatment development [29]. Gamma scintigraphy can be used to measure the distribution of aerosols within the lung [65–68]. The lack of spatial resolution of gamma scintigraphy has generally limited the measurement of the distribution of aerosol deposition to statistical metrics, such as the penetration index (the ratio of peripheral to central deposition), the coefficient of variation, the coefficient of skewness and the quotient between maximum and mean value deposition [66]. For example, Laube et al. (2000) [69] used gamma scintigraphy to measure the penetration index of radio-aerosol in CF patients. The study demonstrated that the penetration index could be manipulated by changing the patient's inspiratory flow rate, but the precise site of deposition with respect to any pathologies present was not determined. PET imaging provides the best regionality and resolution for measurement of deposition distributions [29,70,71]. However, practical challenges limit its widespread use, such as difficulties in producing radiolabeled drug analogues and the very short half-lives of suitable radionuclides [72].

3. Emerging functional imaging

In the previous section, we describe several imaging technologies that have been used extensively for lung imaging. However, there is a need for further advances to address the key shortfalls of the current technology for providing sufficient functional lung imaging capability to address regional lung disease and inhaled treatments. The key will be to deliver sufficient resolution and contrast in the lung, while maintaining a dynamic imaging capability. Over the last decade, synchrotron-based phase-contrast imaging methods have made huge

advances towards this goal. The unique properties of synchrotron radiation are advantageous for imaging within the lung, and translation of these techniques to laboratory-based X-ray sources, and eventually to clinical application promises to provide lung imaging modalities with unprecedented capabilities.

In this section we describe synchrotron-based phase contrast imaging and give examples of its use in the lung. Recent efforts in translation of these technologies to laboratory-based systems are then detailed.

3.1. Phase-contrast imaging

X-ray imaging traditionally utilizes absorption contrast, whereby materials with differing X-ray attenuation properties are differentiated by the intensity of the X-rays that transmit through them onto an X-ray detector. Structures consisting of heavily attenuating materials will appear darker than those containing less attenuating materials. Bone is highly attenuating, and therefore provides high contrast against the surrounding soft tissue. Conversely, the lung parenchyma and surrounding tissue have similar bulk attenuation properties, and thus the lungs generate poor contrast.

Phase-contrast imaging utilizes the difference in refractive properties of materials to generate contrast. Differential changes in the phase of a partially coherent X-ray wave, imparted by different materials in the sample, can be made visible as a consequence of interference with an unperturbed wave. Phase gradients are largest at the boundaries between materials, and hence phase contrast has a predominantly edge enhancing effect.

X-ray sources with high spatial and temporal coherence are required for phase contrast imaging. Synchrotron radiation sources are extremely bright, which enables conditioning of the X-ray beam to create very high coherence while maintaining sufficient flux to image with good temporal resolution. The X-ray energy can be filtered to produce a monochromatic beam to improve temporal coherence, while the distance from the X-ray source to the sample can be increased to reduce the effective spot size and increase spatial coherence [61]. Notwithstanding these advantages, synchrotron radiation sources are highly expensive, and consequently access to these X-ray sources is limited. Therefore, to become widely utilized, the phase contrast imaging technologies developed on the synchrotron must be translated into the laboratory setting, and ultimately to clinical application. Recent developments towards this initial translation to laboratory sized X-ray sources have generated promising results, and widespread laboratory based phase-contrast imaging is now within reach [73–77].

Phase contrast imaging is ideally suited for imaging of the lung, as the many air–tissue interfaces in the lung provide very large X-ray phase gradients. Therefore, phase contrast can provide significant improvements in contrast and detail over absorption based X-ray imaging [61,78–80].

Several methods for generating phase contrast have been applied to the lung, with the two most predominant being grating interferometry and propagation-based imaging (PBI).

3.2. Grating interferometry

Grating interferometry [81,82] uses phase-gratings placed between the sample and detector to generate contrast from the phase changes imparted on the X-ray wave by the sample. These grating are placed between the detector and the sample, effectively resulting in a reduction in efficiency of the system to detect X-rays. To overcome this, very bright X-ray sources, or increased exposure times are required, resulting in a relative increase in X-ray dose imparted to the sample.

Grating interferometry performs well with X-ray sources that exhibit lower coherence, making these methods well-suited for translation from the synchrotron to the lab. Consequently, recent studies have used grating interferometry on a laboratory-based X-ray source [83] with several of these studies relating to lung imaging [84–86].

Schwab et al. [86] demonstrated improved contrast in excised healthy mouse lungs using grating-based imaging on a compact laboratory-based synchrotron. This same imaging setup was also used by Schleede et al. [85] to demonstrate improved diagnosis of emphysema, by comparing the ratio of the phase signal to the attenuation signal, a surrogate marker for alveolar size.

Meinel et al. [84] attempted to use a similar measure on the same setup for improvement of lung cancer detection. Although the preliminary results did not show an increase in sensitivity, delineation of the cancer boundary was improved through the edge enhancing effect.

Grating interferometry shows potential for use in assessing lung function and the effectiveness of inhaled treatments. Although this approach is potentially very sensitive in some cases, the data obtained are structural and thus can only provide anatomical markers for lung health rather than produce functional markers. Furthermore, until temporal resolution is improved dynamic measurements over a breath will not be possible, further limiting utility.

3.3. Propagation-based phase-contrast imaging

The simplest method for generating phase-contrast is propagation-based phase contrast imaging (PBI), sometimes called in-line X-ray phase contrast imaging. By allowing the X-ray wave to propagate a large distance between the sample and detector, interference fringes are generated at the detector plane by the X-ray waves that are slightly refracted at the surface interfaces contained in the sample. The ability to image in phase contrast without gratings or other apparatus between the sample and detector provides a higher efficiency, and therefore increased capability for dynamic imaging [78,87–90]. There have been a number of studies that utilize planar PBI for *in vivo* lung imaging, taking advantage of a simple implementation and capacity for dynamic imaging. For example, Hooper et al. [91] visualized liquid clearance in live newborn rabbit pups as they take their first breaths. Kitchen et al. [92] described a method for calculating ventilation from dynamic imaging of lungs using PBI, demonstrating the possibility for functional metrics to be derived from phase contrast images.

The use of dynamic PBI for investigations into inhaled drug delivery has been demonstrated in several recent studies, and development of image processing and experimental methods stemming from this technology has accelerated in recent years. These studies have exploited the dynamic capabilities of synchrotron PBI in order to probe both the effectiveness of treatments and the efficacy of the delivery methods. Donnelley et al. [93] used high-resolution synchrotron PBI for the detection of inhalable particles in live mouse airways. Subsequent to this, pollutant and other marker particles were used to measure mucociliary transport mechanisms [94]. PBI has been used to measure airway surface liquid depth, specifically for assessment of therapies for cystic fibrosis lung disease [95,96]. Donnelley et al. [97] measured the variability of *in vivo* fluid dose distribution in liquid doses delivered through the pulmonary system. The affect of airway hydrating therapies on mucociliary transport [98,99] has also recently been investigated using synchrotron phase contrast imaging.

3.4. Functional lung imaging using phase contrast

The increased spatial detail and temporal resolution resulting from PBI provides the opportunity to extract quantitative functional information on the lung using advanced image processing methods.

Motion tracking methods, originally developed to measure fluid flow in engineering applications, have been adapted to measure the movement of lung tissue in dynamic PBI images [11]. Expansion of lung tissue is directly linked to air flow into, or out of, regions of the lung, and measurement of the lung expansion can be used to calculate airflow distributions throughout the lung [100], thus adding a functional measurement capability to dynamic X-ray imaging.

Fouras et al. [11] demonstrated that motion of lung tissue alters dramatically in the presence of lung injury, providing improved sensitivity and earlier detection of disease over other methods.

Dubsky et al. [100] developed a method for 4D dynamic measurements of airflow throughout the entire lung (Fig. 4). This method can provide both regional functional information for disease detection or assessment of treatments, and also high quality functional inputs for computational modeling. This method has been shown to improve accuracy and sensitivity for detection of cystic fibrosis lung disease over spirometric methods [26]. This method is based on 4DCT, and therefore imparts significant dose to the subject. However, our research group has also developed a novel method that can reduce the dose by orders of magnitudes, allowing 4D measurement of lung motion from as few as 6 images [101–103] (Fig. 5). By producing functional images without the requirement for phase gating, as in 4DCT, this method can measure short-lived effects, significantly broadening the scope of treatments and conditions that can be assessed, particularly for investigations into inhaled treatments for which the functional effects are often transient.

Functional lung imaging using phase-contrast has been demonstrated to outperform current imaging methods for the assessment of disease and treatments. However, the requirement for synchrotron radiation severely limits its widespread adoption. In order to fully realize the potential in this field, translation from the synchrotron to the laboratory, and then into the clinic, is critical.

3.5. Laboratory propagation-based phase-contrast imaging

Almost 20 years ago, it was demonstrated that PBI could be performed on a laboratory source with sufficient spatial coherence [104]. However, only recent developments in X-ray source technology have enabled this method to achieve sufficient temporal resolution to be useful for lung imaging. The challenge lies in creating an X-ray source that provides adequate power while maintaining a source spot size small enough to deliver the required spatial coherence.

Garson et al. [105] demonstrated that lung images of similar quality to those acquired at a synchrotron can be produced using laboratory-based sources. However, the relatively low power of the X-ray source used resulted in exposure times that are too long for dynamic or *in vivo* studies.

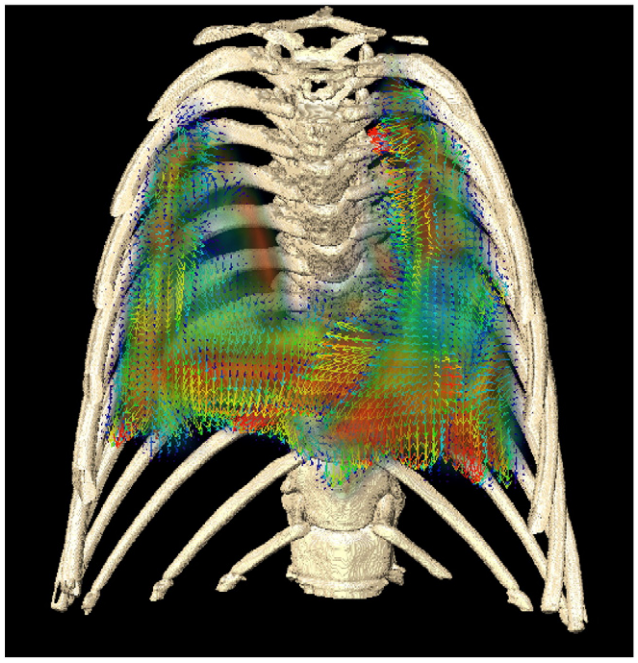

Fig. 5. Computed tomographic X-ray velocimetry reconstruction of lung motion. Vectors show speed and direction of lung tissue of a mouse during inspiration. Motion field was reconstructed using computed tomographic X-ray velocimetry from 6 images (3 simultaneously captured views at two-time points) acquired using liquid-metal jet X-ray sources. Skeletal information is acquired from a co-registered high-resolution CT.

Recently, the development of liquid-metal-jet X-ray sources opens up the possibility for dynamic PBI in the laboratory. These X-ray sources provide unparalleled brightness for small spot sizes, allowing for very high quality phase contrast imaging with reduced exposure times [75]. Use of the liquid-metal-jet source for PBI has been demonstrated in a number of applications, including for high-resolution angiography [76] and cancer demarcation in small animals [77].

It has recently been demonstrated that successful high-resolution dynamic phase-contrast *in vivo* lung imaging can be effected using a liquid-metal-jet laboratory X-ray source (Excillum, D2) [74]. Using

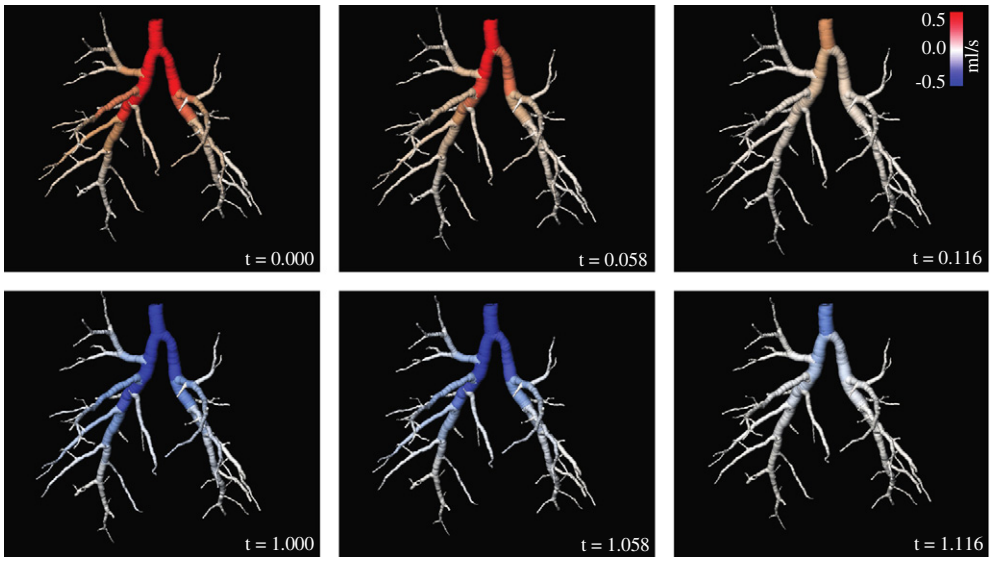

Fig. 4. Distribution of flow throughout the airway tree, measured using functional lung imaging. Instantaneous flow of air through the rabbit pup airway tree at six time points (from sequence of 20 timepoints) during ventilation. Positive flow (red) indicates inspiratory flow and negative flow (blue) indicates expiratory flow [100].

this new technology, translation of functional dynamic phase-contrast imaging from the synchrotron the laboratory is within reach, and the full potential of these methods will be realized in the near future.

4. Conclusions

Respiratory infection has significant regional effects on lung function. Additionally, the efficacy of treatment delivered through inhalation is strongly influenced by regional lung function. This feedback loop must be understood in detail for accurate assessment of new and developing treatments and delivery systems. This requires advancement of functional lung imaging beyond the currently available methods to improve both spatial and temporal resolution.

We have identified three critical unmet needs for functional lung imaging in the field of respiratory infection: (1) regional assessment of functional consequences of pathology, and (2) regional assessment of response to inhaled treatment, and (3) input into deposition modeling studies.

No established imaging modalities can provide high-resolution functional measurements to adequately address these needs. Emerging methods based on synchrotron phase contrast imaging have the potential to fulfill these requirements, and a recent trend of translation to laboratory applications and into the clinical setting offers enticing possibilities beyond research into treatments and inhaled delivery methods. There also exists the potential for functional lung imaging to become core to the treatment process. The capacity to provide accurate regional assessment of disease, and patient specific deposition modeling, opens the possibility of sophisticated tailoring of inhaled treatment parameters (size of particles, concentration, inspiratory flow rate) in order to target the most diseased areas. Additionally, these parameters can be effectively adapted over the course of the treatment as the patient's function changes and improves. This full integration of imaging and modeling as a companion diagnostic to antibiotic treatment has the potential to dramatically improve efficiency and effectiveness of inhaled treatments, leading to substantially improved patient outcomes.

Acknowledgments

The authors are supported by the National Health and Medical Research Council (AF & SD: Development Grant APP1055116, AF: Career Development Fellowship APP1022721), and the Multi-modal Australian ScienceS Imaging and Visualisation Environment (MASSIVE; www.massive.org.au). We thank Rajeev Samarage for assistance in figure preparation.

References

[1] H.T. Robertson, R.B. Buxton, Imaging for lung physiology: what do we wish we could measure? J. Appl. Physiol. (2012) 317–327.
[2] A. Fouras, S. Dubsky, The role of functional lung imaging in improvement of pulmonary drug delivery, in: A. Nokhodchi, G.P. Martin (Eds.), Pulmonary Drug Delivery: Advances and Challenges, Wiley-Blackwell, 2015.
[3] J.H. Bates, Lung Mechanics: An Inverse Modeling Approach, Cambridge University Press, 2009.
[4] E.R. Weibel, What makes a good lung? Swiss Med. Wkly. 139 (2009) 375–386.
[5] J.G. Venegas, T. Winkler, G. Musch, M.F.V. Melo, D. Layfield, N. Tgavalekos, A.J. Fischman, R.J. Callahan, G. Bellani, R.S. Harris, Self-organized patchiness in asthma as a prelude to catastrophic shifts, Nature 434 (2005) 777–782.
[6] T. Winkler, J.G. Venegas, Complex airway behavior and paradoxical responses to bronchoprovocation, J. Appl. Physiol. (2007) 655–663.
[7] J. Venegas, T. Winkler, G. Musch, M. Melo, D. Layfield, N. Tgavalekos, A. Fischman, R. Callahan, G. Bellani, R. Harris, Self-organized patchiness in asthma as a prelude to catastrophic shifts, Nature (2005) 777–782.
[8] T. Winkler, J.G. Venegas, Self-organized patterns of airway narrowing, J. Appl. Physiol. (2011) 1482–1486.
[9] S. Bayat, L. Porra, H. Suhonen, P. Suortti, A.R.A. Sovijarvi, Paradoxical conducting airway responses and heterogeneous regional ventilation after histamine inhalation in rabbit studied by synchrotron radiation CT, J. Appl. Physiol. (2009) 1949–1958.
[10] S. Bayat, Ventilation heterogeneity: small length scales, big challenges, J. Appl. Physiol. (1985) 113 (2012) 851–852.
[11] A. Fouras, B.J. Allison, M.J. Kitchen, S. Dubsky, J. Nguyen, K. Hourigan, K.K.W. Siu, R.A. Lewis, M.J. Wallace, S.B. Hooper, Altered lung motion is a sensitive indicator of regional lung disease, Ann. Biomed. Eng. 40 (2012) 1160–1169.
[12] R.S. Harris, H. Fujii-Rios, T. Winkler, G. Musch, M.F. Vidal Melo, J.G. Venegas, Ventilation defect formation in healthy and asthma subjects is determined by lung inflation, Plos ONE (2012) e53216.
[13] G. Musch, J.D.H. Layfield, R.S. Harris, M.F.V. Melo, T. Winkler, R.J. Callahan, A.J. Fischman, J.G. Venegas, Topographical distribution of pulmonary perfusion and ventilation, assessed by PET in supine and prone humans, J. Appl. Physiol. 93 (2002) 1841–1851.
[14] N.T. Tgavalekos, G. Musch, R.S. Harris, M.F. Vidal Melo, T. Winkler, T. Schroeder, R. Callahan, K.R. Lutchen, J.G. Venegas, Relationship between airway narrowing, patchy ventilation and lung mechanics in asthmatics, Eur. Respir. J. (2007) 1174–1181.
[15] H.E. Fessler, S.M. Scharf, E.P. Ingenito, R.J. McKenna, A. Sharafkhaneh, Physiologic basis for improved pulmonary function after lung volume reduction, Proc. Am. Thorac. Soc. (2008) 416–420.
[16] J. Brieland, P. Freeman, R. Kunkel, C. Chrisp, M. Hurley, J. Fantone, C. Engleberg, Replicative *Legionella pneumophila* lung infection in intratracheally inoculated A/J mice. A murine model of human Legionnaires' disease, Am. J. Pathol. 7 (1994) 1537–1546.
[17] M. Berger, Inflammation in the lung in cystic fibrosis. A vicious cycle that does more harm than good? Clin. Rev. Allergy (1991) 119–142.
[18] J.R. Starke, M.S. Edwards, C. Langston, C.J. Baker, A mouse model of chronic pulmonary infection with *Pseudomonas aeruginosa* and *Pseudomonas cepacia*, Pediatr. Res. (1987) 698–702.
[19] M. Tam, G.J. Snipes, M.M. Stevenson, Characterization of chronic bronchopulmonary *Pseudomonas aeruginosa* infection in resistant and susceptible inbred mouse strains, Am. J. Respir. Cell Mol. (1999) 710–719.
[20] F. Wolbeling, A. Munder, F. Stanke, B. Tummler, U. Baumann, Head-out spirometry accurately monitors the course of *Pseudomonas aeruginosa* lung infection in mice, Respiration 80 (2010) 340–346.
[21] F. Wolbeling, A. Munder, T. Kerber-Momot, D. Neumann, C. Hennig, G. Hansen, B. Tummler, U. Baumann, Lung function and inflammation during murine *Pseudomonas aeruginosa* airway infection, Immunobiology 216 (2011) 901–908.
[22] A. Munder, S. Krusch, T. Tschernig, M. Dorsch, A. Lührmann, M. van Griensven, B. Tümmler, S. Weiss, H.J. Hedrich, Pulmonary microbial infection in mice: comparison of different application methods and correlation of bacterial numbers and histopathology, Exp. Toxicol. Pathol. (2002) 127–133.
[23] S. Sethi, T.F. Murphy, Current concepts: infection in the pathogenesis and course of chronic obstructive pulmonary disease, N. Engl. J. Med. 359 (2008) 2355–2365.
[24] E. Monso, J. Ruiz, A. Rosell, J. Manterola, J. Fiz, J. Morera, V. Ausina, Bacterial infection in chronic obstructive pulmonary disease. A study of stable and exacerbated outpatients using the protected specimen brush, Am. J. Respir. Crit. Care Med. (1995) 1316–1320.
[25] H.A.W.M. Tiddens, A.C. Bos, J.W. Mouton, S. Devadason, H.M. Janssens, Inhaled antibiotics: dry or wet? Eur. Respir. J. 44 (2014) 1308–1318.
[26] C.S. Stahr, C.R. Samarage, D.W. Parsons, S. Dubsky, M. Donnelley, J. Thurgood, Y. Henon, K.K.W. Siu, A. Fouras, Regional Image Based Pulmonary Function Testing Detects CF Lung Disease Earlier Than Conventional PFT, B38, Update in Adult Cystic Fibrosis, American Thoracic Society, 2014. pp. A2837-A2837.
[27] A.C. Bos, W.G. Vos, J.W. de Backer, C. van Holsbeke, H.M. Janssens, H.A.W.M. Tiddens, 196 Airway surface liquid concentrations of aztreonam lysine for inhalation in children with cystic fibrosis: a modelling study, J. Cyst. Fibros. (2013) S98.
[28] S.-A. Ricketts, P.D. Hockings, J.C. Waterton, Non-Invasive Imaging in the Pharmaceutical Industry, Springer Berlin Heidelberg, Berlin, Heidelberg, 2011. 17–27.
[29] J. Conway, Lung imaging—two dimensional gamma scintigraphy, SPECT, CT and PET, Adv. Drug Deliv. Rev. (2012) 1–12.
[30] R. Mead-Hunter, A.J.C. King, A.N. Larcombe, B.J. Mullins, The influence of moving walls on respiratory aerosol deposition modelling, J. Aerosol Sci. (2013) 1–23.
[31] W.A. Wall, T. Rabczuk, Fluid–structure interaction in lower airways of CT-based lung geometries, Int. J. Numer. Methods Fluids 57 (2008) 653–675.
[32] G. Xia, M.H. Tawhai, E.A. Hoffman, C.-L. Lin, Airway wall stiffening increases peak wall shear stress: a fluid–structure interaction study in rigid and compliant airways, Ann. Biomed. Eng. 38 (2010) 1836–1853.
[33] J.W. De Backer, W.G. Vos, S.C. Vinchurkar, R. Claes, A. Drollmann, D. Wulfrank, P.M. Parizel, P. Germonpré, W. De Backer, Validation of computational fluid dynamics in CT-based airway models with SPECT/CT, Radiology 257 (2010) 854–862.
[34] W. De Backer, A. Devolder, G. Poli, D. Acerbi, R. Monno, C. Herpich, K. Sommerer, T. Meyer, F. Mariotti, Lung deposition of BDP/formoterol HFA pMDI in healthy volunteers, asthmatic, and COPD patients, J. Aerosol Med. Pulm. Drug Deliv. 23 (2010) 137–148.
[35] K. Inthavong, L.-T. Choi, J. Tu, S. Ding, F. Thien, Micron particle deposition in a tracheobronchial airway model under different breathing conditions, Med. Eng. Phys. 32 (2010) 1198–1212.
[36] A.R. Lambert, P. O'Shaughnessy, M.H. Tawhai, E.A. Hoffman, C.-L. Lin, Regional deposition of particles in an image-based airway model: large-eddy simulation and left–right lung ventilation asymmetry, Aerosol Sci. Technol. 45 (2011) 11–25.
[37] S. Vinchurkar, L. De Backer, W. Vos, C. Van Holsbeke, J. De Backer, W. De Backer, A case series on lung deposition analysis of inhaled medication using functional imaging based computational fluid dynamics in asthmatic patients: effect of upper airway morphology and comparison with in vivo data, Inhal. Toxicol. 24 (2012) 81–88.

[38] T. Xiong, H. Ilmi, Y. Hoarau, P. Choquet, C. Goetz, A. Fouras, S. Dubsky, M. Braza, S. Sainlos-Brillac, F. Plouraboue, D. Lo Jacono, Flow and particles deposition in anatomically realistic airways, Comput. Methods Biomech. Biomed. Engin. 15 (2012) 56–58.
[39] A. Kak, M. Slaney, Principles of Computerized Tomographic Imaging, Society for Industrial and Applied Mathematics, 2001.
[40] D.J. Brenner, E.J. Hall, Current concepts—computed tomography—an increasing source of radiation exposure, N. Engl. J. Med. 357 (2007) 2277–2284.
[41] J.M. Reinhardt, K. Ding, K. Cao, G.E. Christensen, E.A. Hoffman, S.V. Bodas, Registration-based estimates of local lung tissue expansion compared to xenon CT measures of specific ventilation, Med. Image Anal. (2008) 752–763.
[42] B.A. Simon, Regional ventilation and lung mechanics using X-ray CT, Acad. Radiol. 12 (2005) 1414–1422.
[43] C.J. Galbán, M.K. Han, J.L. Boes, K.A. Chughtai, C.R. Meyer, T.D. Johnson, S. Galbán, A. Rehemtulla, E.A. Kazerooni, F.J. Martinez, B.D. Ross, Computed tomography-based biomarker provides unique signature for diagnosis of COPD phenotypes and disease progression, Nat. Med. 18 (2012) 1711–1715.
[44] E. De Langhe, G. Vande Velde, J. Hostens, U. Himmelreich, B. Nemery, F.P. Luyten, J. Vanoirbeek, R.J. Lories, Quantification of lung fibrosis and emphysema in mice using automated micro-computed tomography, Plos ONE 7 (2012) e43123.
[45] M.O. Wielputz, M. Eichinger, Z. Zhou, K. Leotta, S. Hirtz, S.H. Bartling, W. Semmler, H.U. Kauczor, M. Puderbach, M.A. Mall, In vivo monitoring of cystic fibrosis-like lung disease in mice by volumetric computed tomography, Eur. Respir. J. (2011) 1060–1070.
[46] S. Kobayashi, R. Fujinawa, F. Ota, S. Kobayashi, T. Angata, M. Ueno, T. Maeno, S. Kitazume, K. Yoshida, T. Ishii, C. Gao, K. Ohtsubo, Y. Yamaguchi, T. Betsuyaku, K. Kida, N. Taniguchi, A single dose of lipopolysaccharide into mice with emphysema mimics human chronic obstructive pulmonary disease exacerbation as assessed by micro-computed tomography, Am. J. Respir. Cell Mol. (2013) 971–977.
[47] G.E. Christensen, J.H. Song, W. Lu, I. El Naqa, D.A. Low, Tracking lung tissue motion and expansion/compression with inverse consistent image registration and spirometry, Med. Phys. 34 (2007) 2155–2163.
[48] K. Ding, J.E. Bayouth, J.M. Buatti, G.E. Christensen, J.M. Reinhardt, 4DCT-based measurement of changes in pulmonary function following a course of radiation therapy, Med. Phys. 37 (2010) 1261–1272.
[49] J.M. Reinhardt, K. Ding, K. Cao, G.E. Christensen, E.A. Hoffman, S.V. Bodas, Registration-based estimates of local lung tissue expansion compared to xenon CT measures of specific ventilation, Med. Image Anal. 12 (2008) 752–763.
[50] Y. Yin, J. Choi, E.A. Hoffman, M.H. Tawhai, C.-L. Lin, Simulation of pulmonary air flow with a subject-specific boundary condition, J. Biomech. 43 (2010) 2159–2163.
[51] R. Castillo, E. Castillo, J. Martinez, T. Guerrero, Ventilation from four-dimensional computed tomography: density versus Jacobian methods, Phys. Med. Biol. 55 (2010) 4661–4685.
[52] T. Guerrero, K. Sanders, E. Castillo, Y. Zhang, L. Bidaut, T. Pan, R. Komaki, Dynamic ventilation imaging from four-dimensional computed tomography, Phys. Med. Biol. 51 (2006) 777–791.
[53] T. Pan, T.-Y. Lee, E. Rietzel, G.T.Y. Chen, 4D-CT imaging of a volume influenced by respiratory motion on multi-slice CT, Med. Phys. 31 (2004) 333–340.
[54] T. Yamamoto, S. Kabus, T. Klinder, C. Lorenz, J. von Berg, T. Blaffert, B.W. Loo Jr., P.J. Keall, Investigation of four-dimensional computed tomography-based pulmonary ventilation imaging in patients with emphysematous lung regions, Phys. Med. Biol. 56 (2011) 2279–2298.
[55] M. Ebert, T. Grossmann, W. Heil, W. Otten, R. Surkau, M. Leduc, P. Bachert, M. Knopp, L. Schad, M. Thelen, Nuclear magnetic resonance imaging with hyperpolarised helium-3, Lancet 347 (1996) 1297–1299.
[56] K. Emami, M. Stephen, S. Kadlecek, R.V. Cadman, M. Ishii, R.R. Rizi, Quantitative assessment of lung using hyperpolarized magnetic resonance imaging, Proc. Am. Thorac. Soc. 6 (2009) 431–438.
[57] K.R. Dunster, M.E.J. Friese, J.F. Fraser, G.J. Galloway, G.J. Cowin, A. Schibler, Ventilation distribution in rats: part 2—a comparison of electrical impedance tomography and hyperpolarised helium magnetic resonance imaging, Biomed. Eng. Online 11 (2012) 68.
[58] M. Cheney, D. Isaacson, J.C. Newell, Electrical impedance tomography, SIAM Rev. 41 (1999) 85–101.
[59] I. Frerichs, Electrical impedance tomography (EIT) in applications related to lung and ventilation: a review of experimental and clinical activities, Physiol. Meas. 21 (2000) R1–R21.
[60] J. Victorino, J. Borges, V. Okamoto, G. Matos, M. Tucci, M. Caramez, H. Tanaka, F. Sipmann, D. Santos, C. Barbas, C. Carvalho, M. Amato, Imbalances in regional lung ventilation—a validation study on electrical impedance tomography, Am. J. Respir. Crit. Care 169 (2004) 791–800.
[61] A. Fouras, M.J. Kitchen, S. Dubsky, R.A. Lewis, S.B. Hooper, K. Hourigan, The past, present, and future of X-ray technology for in vivo imaging of function and form, J. Appl. Phys. 105 (2009) 102009.
[63] R.S. Harris, D.P. Schuster, Visualizing lung function with positron emission tomography, J. Appl. Physiol. 102 (2006) 448–458.
[64] B.N. Jobse, R.G. Rhem, C.A.J.R. McCurry, I.Q. Wang, N.R. Labiris, Imaging lung function in mice using SPECT/CT and per-voxel analysis, Plos ONE 7 (2012) e42187.
[65] S. Warren, G. Taylor, J. Smith, H. Buck, M. Parry-Billings, Gamma scintigraphic evaluation of a novel budesonide dry powder inhaler using a validated radiolabeling technique, J. Aerosol Med. (2002) 15–25.
[66] L. Olséni, J. Palmer, P. Wollmer, Quantitative evaluation of aerosol deposition pattern in the lung in patients with chronic bronchitis, Physiol. Meas. (1994) 41–48.
[67] B.L. Laube, J.M. Links, N.D. LaFrance, H.N. Wagner, B.J. Rosenstein, Homogeneity of bronchopulmonary distribution of 99mTc aerosol in normal subjects and in cystic fibrosis patients, Chest (1989) 822–830.
[68] E. Bondesson, T. Bengtsson, L. Borgström, L.-E. Nilsson, K. Norrgren, E. Trofast, P. Wollmer, Planar gamma scintigraphy—points to consider when quantifying pulmonary dry powder aerosol deposition, Int. J. Pharm. (2003) 33–47.
[69] B.L. Laube, R. Jashnani, R.N. Dalby, P.L. Zeitlin, Targeting aerosol deposition in patients with cystic fibrosis: effects of alterations in particle size and inspiratory flow rate, Chest (2000) 1069–1076.
[70] M. Yanai, J. Hatazawa, F. Ojima, H. Sasaki, M. Itoh, T. Ido, Deposition and clearance of inhaled ^{18}FDG powder in patients with chronic obstructive pulmonary disease, Eur. Respir. J. (1998) 1342–1348.
[71] M.B. Dolovich, 18F-fluorodeoxyglucose positron emission tomographic imaging of pulmonary functions, pathology, and drug delivery, Proc. Am. Thorac. Soc. (2009) 477–485.
[72] S. Newman, J. Fleming, Challenges in assessing regional distribution of inhaled drug in the human lungs, Expert Opin. Drug Deliv. 8 (2011) 841–855.
[73] M. Bech, A. Tapfer, A. Velroyen, A. Yaroshenko, B. Pauwels, J. Hostens, P. Bruyndonckx, A. Sasov, F. Pfeiffer, In-vivo dark-field and phase-contrast X-ray imaging, Sci. Rep. 3 (2013) 3209.
[74] S. Dubsky, J. Thurgood, Y. Henon, A. Fouras, A Low Dose, High Spatio-temporal Resolution System for Real-Time Four-Dimensional Lung Function Imaging, C36, Imaging and the Lung: A Rapidly Evolving Field, American Thoracic Society, 2014. pp. A4316-A4316.
[75] T. Tuohimaa, M. Otendal, H.M. Hertz, Phase-contrast X-ray imaging with a liquid-metal-jet-anode microfocus source, Appl. Phys. Lett. 91 (2007) 074104.
[76] U. Lundström, D.H. Larsson, A. Burvall, P.A.C. Takman, L. Scott, H. Brismar, H.M. Hertz, X-ray phase contrast for CO_2 microangiography, Phys. Med. Biol. 57 (2012) 2603–2617.
[77] D.H. Larsson, U. Lundström, U.K. Westermark, M. Arsenian Henriksson, A. Burvall, H.M. Hertz, First application of liquid-metal-jet sources for small-animal imaging: high-resolution CT and phase-contrast tumor demarcation, Med. Phys. 40 (2013) 021909.
[78] R. Lewis, N. Yagi, M. Kitchen, M. Morgan, D. Paganin, K. Siu, K. Pavlov, I. Williams, K. Uesugi, M. Wallace, C. Hall, J. Whitley, S. Hooper, Dynamic imaging of the lungs using X-ray phase contrast, Phys. Med. Biol. 50 (2005) 5031–5040.
[79] M.L. Siew, A.B. Te Pas, M.J. Wallace, M.J. Kitchen, M.S. Islam, R.A. Lewis, A. Fouras, C.J. Morley, P.G. Davis, N. Yagi, K. Uesugi, S.B. Hooper, Surfactant increases the uniformity of lung aeration at birth in ventilated preterm rabbits, Pediatr. Res. 70 (2011) 50–55.
[80] M.J. Kitchen, A. Habib, A. Fouras, S. Dubsky, R.A. Lewis, M.J. Wallace, S.B. Hooper, A new design for high stability pressure-controlled ventilation for small animal lung imaging, J. Instrum. 5 (2010) T02002.
[81] T. Weitkamp, A. Diaz, C. David, F. Pfeiffer, M. Stampanoni, P. Cloetens, E. Ziegler, X-ray phase imaging with a grating interferometer, Opt. Express 13 (2005) 6296–6304.
[82] P. Zhu, K. Zhang, Z. Wang, Y. Liu, X. Liu, Z. Wu, S.A. McDonald, F. Marone, M. Stampanoni, Low-dose, simple, and fast grating-based X-ray phase-contrast imaging, Proc. Natl. Acad. Sci. 107 (2010) 13576–13581.
[83] A. Tapfer, M. Bech, A. Velroyen, J. Meiser, J. Mohr, M. Walter, J. Schulz, B. Pauwels, P. Bruyndonckx, X. Liu, A. Sasov, F. Pfeiffer, Experimental results from a preclinical X-ray phase-contrast CT scanner, Proc. Natl. Acad. Sci. 109 (2012) 15691–15696.
[84] F.G. Meinel, F. Schwab, A. Yaroshenko, A. Velroyen, M. Bech, K. Hellbach, J. Fuchs, T. Stiewe, A.Ö. Yildirim, F. Bamberg, M.F. Reiser, F. Pfeiffer, K. Nikolaou, Lung tumors on multimodal radiographs derived from grating-based X-ray imaging—a feasibility study, Phys. Med. (2013) 1–6.
[85] S. Schleede, F.G. Meinel, M. Bech, J. Herzen, K. Achterhold, G. Potdevin, A. Malecki, S. Adam-Neumair, S.F. Thieme, F. Bamberg, K. Nikolaou, A. Bohla, A.Ö. Yildirim, R. Loewen, M. Gifford, R. Ruth, O. Eickelberg, M. Reiser, F. Pfeiffer, Emphysema diagnosis using X-ray dark-field imaging at a laser-driven compact synchrotron light source, Proc. Natl. Acad. Sci. 109 (2012) 17880–17885.
[86] F. Schwab, S. Schleede, D. Hahn, M. Bech, J. Herzen, S. Auweter, F. Bamberg, K. Achterhold, A.Ö. Yildirim, A. Bohla, O. Eickelberg, R. Loewen, M. Gifford, R. Ruth, M.F. Reiser, K. Nikolaou, F. Pfeiffer, F.G. Meinel, Comparison of contrast-to-noise ratios of transmission and dark-field signal in grating-based X-ray imaging for healthy murine lung tissue, Z. Med. Phys. 23 (2013) 236–242.
[87] R.P. Murrie, A.W. Stevenson, K.S. Morgan, A. Fouras, D.M. Paganin, K.K.W. Siu, Feasibility study of propagation-based phase-contrast X-ray lung imaging on the Imaging and Medical beamline at the Australian Synchrotron, J. Synchrotron Radiat. 21 (2014) 430–445, http://dx.doi.org/10.1107/S1600577513034681 (International Union of Crystallography, 2014, pp. 1–16).
[88] S.C. Irvine, D.M. Paganin, A. Jamison, S. Dubsky, A. Fouras, Vector tomographic X-ray phase contrast velocimetry utilizing dynamic blood speckle, Opt. Express 18 (2010) 2368–2379.
[89] R.A. Jamison, S. Dubsky, K.K. Siu, K. Hourigan, A. Fouras, X-ray velocimetry and haemodynamic forces within a stenosed femoral model at physiological flow rates, Ann. Biomed. Eng. 39 (2011) 1643–1653.
[90] R.A. Jamison, K.K. Siu, S. Dubsky, J.A. Armitage, A. Fouras, X-ray velocimetry within the ex vivo carotid artery, J. Synchrotron Radiat. 19 (2012) 1050–1055.
[91] S.B. Hooper, M.J. Kitchen, M.L. Siew, R.A. Lewis, A. Fouras, A.B. te Pas, K.K. Siu, N. Yagi, K. Uesugi, M.J. Wallace, Imaging lung aeration and lung liquid clearance at birth using phase contrast x-ray imaging, Clin. Exp. Pharmacol. Physiol. 36 (2009) 117–125.
[92] M.J. Kitchen, R.A. Lewis, M.J. Morgan, M.J. Wallace, M.L. Siew, K.K.W. Siu, A. Habib, A. Fouras, N. Yagi, K. Uesugi, S.B. Hooper, Dynamic measures of regional lung air volume using phase contrast X-ray imaging, Phys. Med. Biol. 53 (2008) 6065–6077.

[93] M. Donnelley, K.S. Morgan, A. Fouras, W. Skinner, K. Uesugi, N. Yagi, K.K.W. Siu, D.W. Parsons, Real-time non-invasive detection of inhalable particulates delivered into live mouse airways, J. Synchrotron Radiat. 16 (2009) 553–561.
[94] M. Donnelley, K.S. Morgan, K.K.W. Siu, D.W. Parsons, Dry deposition of pollutant and marker particles onto live mouse airway surfaces enhances monitoring of individual particle mucociliary transit behaviour, J. Synchrotron Radiat. 19 (2012) 551–558.
[95] K.S. Morgan, M. Donnelley, D.M. Paganin, A. Fouras, N. Yagi, Y. Suzuki, A. Takeuchi, K. Uesugi, R.C. Boucher, D.W. Parsons, K.K.W. Siu, Measuring airway surface liquid depth in ex vivo mouse airways by X-ray imaging for the assessment of cystic fibrosis airway therapies, Plos ONE 8 (2013) e55822.
[96] K.S. Morgan, M. Donnelley, N. Farrow, A. Fouras, N. Yagi, Y. Suzuki, A. Takeuchi, K. Uesugi, R.C. Boucher, K.K.W. Siu, D.W. Parsons, In vivo X-ray imaging reveals improved airway surface hydration after a therapy designed for cystic fibrosis, Am. J. Respir. Crit. Care (2014) 469–471.
[97] M. Donnelley, K.S. Morgan, K.K.W. Siu, D.W. Parsons, Variability of in vivo fluid dose distribution in mouse airways is visualized by high-speed synchrotron X-ray imaging, J. Aerosol Med. Pulm. Drug Deliv. 26 (2013) 307–316.
[98] M. Donnelley, K.S. Morgan, K.K.W. Siu, N.R. Farrow, C.S. Stahr, R.C. Boucher, A. Fouras, D.W. Parsons, Non-invasive airway health assessment: synchrotron imaging reveals effects of rehydrating treatments on mucociliary transit in-vivo, Sci. Rep. 4 (2014) 3689.
[99] M. Donnelley, K.S. Morgan, K.K. Siu, A. Fouras, N.R. Farrow, R.P. Carnibella, D.W. Parsons, Tracking extended mucociliary transport activity of individual deposited particles: longitudinal synchrotron X-ray imaging in live mice, J. Synchrotron Radiat. 21 (2014) 768–773, http://dx.doi.org/10.1107/S160057751400856X (International Union of Crystallography, 2014, pp. 1–6).
[100] S. Dubsky, S.B. Hooper, K.K.W. Siu, A. Fouras, Synchrotron-based dynamic computed tomography of tissue motion for regional lung function measurement, J. R. Soc. Interface 9 (2012) 2213–2224.
[101] S. Dubsky, S.B. Hooper, K. Siu, In vivo tomographic velocimetry of the lung for the detailed study of lung disease and its treatments, SPIE Optical2012.
[102] S. Dubsky, R.A. Jamison, S.P.A. Higgins, K.K.W. Siu, K. Hourigan, A. Fouras, Computed tomographic X-ray velocimetry for simultaneous 3D measurement of velocity and geometry in opaque vessels, Exp. Fluids 52 (2010) 543–554.
[103] S. Dubsky, R.A. Jamison, S.C. Irvine, K.K.W. Siu, K. Hourigan, A. Fouras, Computed tomographic X-ray velocimetry, Appl. Phys. Lett. 96 (2010) 023702.
[104] S.W. Wilkins, T.E. Gureyev, D. Gao, A. Pogany, A.W. Stevenson, Phase-contrast imaging using polychromatic hard X-rays, Nature 384 (1996) 335–338.
[105] A.B. Garson III, E.W. Izaguirre, S.G. Price, M.A. Anastasio, Characterization of speckle in lung images acquired with a benchtop in-line X-ray phase-contrast system, Phys. Med. Biol. 58 (2013) 4237–4253.